ELECTROPERMEABILIZATION FOR ORGANIC MATERIAL – NUMERICAL MODELING

FLORIN SĂFTOIU¹, ALEXANDRU MOREGA², YELDA VELI²

Keywords: Electropermeabilization (EP); Electric field; Electric conductivity; Heat transfer; Finite element method (FEM).

Electroporation, also known as electropermeabilization (EP), occurs when a cell's transmembrane potential exceeds a critical threshold under the influence of an electric field, corresponding to a limit value of the electric field intensity. EP depends on the distribution of the electric field, which in turn depends on and, here, determines the material's electrical properties. Some critical electric field strengths act as a "switch" for the EP, which is, to some extent, reversible. This paper aims, through numerical experiments, to unveil the effects of the electric field on the poration of an organic substance (lavender) and the thermal stability of the EP cell. The substance is assumed to be a continuous medium with electric-field-dependent material properties.

1. INTRODUCTION

In process engineering, solid-liquid extraction is a mass transfer phenomenon driven by the difference in chemical potential between the solid matrix and the solvent. The process can be described as a combination of molecular diffusion, pore diffusion, and convection, being influenced by parameters such as concentration gradient, diffusion coefficient, cell membrane permeability, and solvent properties (polarity, viscosity, surface tension). Traditionally, extraction was accelerated by increasing temperature or mechanical methods, but these methods posed the risk of degrading thermosensitive compounds and losing volatile compounds. The appearance of membrane pores alters the system's (cell's) structure and electrical properties [1,2].

Poration or permeabilization refers to the formation of membrane micropores that increase in diameter until they stabilize as absorbent pores. Pore formation increases the permeability of the cell membrane, allowing impermeable substances to cross the membrane barrier. Thus, extracellular compounds can access the cell interior, and intracellular components can leave the cell and even cause cell death through loss of homeostasis [1–3]. Fields such as medicine, chemistry, and nutrition are already using this technique to improve or even replace traditional methods.

Electroporation (EP) has multiple promising applications in biotechnology, including modifying the permeability of cell membranes by applying an electric field. Among the primary applications are the genetic transformation of microorganisms (electro-transformation), which enables the introduction of foreign DNA into cells to produce valuable biomolecules, such as enzymes or hormones. EP is also used to inactivate microorganisms, being effective for decontaminating wastewater or pasteurizing food without affecting their quality. Another important application is the extraction of biomolecules (electroextraction), where electroporation facilitates the recovery of DNA, proteins, and lipids from microorganisms without the use of aggressive chemicals. The technique is also applied in industrial processes such as biomass drying, reducing energy consumption, and accelerating the process. The integration of electroporation into microfluidic systems opens new possibilities in small-scale cellular manipulation and analysis [3,4].

2. MODELLING THE EP PROCESS

EP is a dynamic regime problem, non-stationary diffusion, described by the laws of the electromagnetic field. Under the

given conditions, at the working frequency, the displacement electric current is negligibly small compared to the conduction electric current density. Therefore, the mathematical model of the EP in a pulsed electric field is described by

$$rot \mathbf{E} = -\frac{\partial \mathbf{B}}{\partial t'}$$
 Faraday's law, (1)

$$div \mathbf{J} = 0$$
, electric charge conservation, (2)

$$rot \mathbf{H} = \mathbf{J} + \mathbf{J}_d$$
, magnetic circuit law, (3)

$$div \mathbf{B} = 0$$
, magnetic flux law, (4)

 $I = \sigma(E)E$

$$\mathbf{B} = \mu_0 \mathbf{H}$$
, constitutive laws. (5)

$$\mathbf{D} = \varepsilon(\mathbf{E})\mathbf{E}$$

where **E** [V/m] is the electric field strength, **B** [T] is the magnetic flux density, **J** [A/m²] is the conduction electric current density, $\mathbf{J}_d = -\partial \mathbf{D} / \partial t$ is the displacement current density, $\sigma(\mathbf{E})$ [S/m] is the electrical conductivity, **D** [C/m²] is the electric flux density, **H** [A/m] is the magnetic field strength, μ_0 [H/m] is the magnetic permeability, and ϵ [F/m] is the electrical permittivity.

The electrical permittivity and electrical conductivity are assumed to be invariant here, but they depend on the phase of the organic matter – permeabilized or not. There is a threshold electric field intensity (electric potential gradient), $\mathbf{E}_{\text{critic}}$, above which the electrical conductivity jumps.

Under these conditions, at the working frequency, the J_d is negligibly small compared to the J, so that the mathematical model of the EP in a pulsed electric field, described by eq. (1) to eq. (5), is given by

$$-\nabla \cdot \left(\varepsilon \frac{\partial V}{\partial t}\right) - \nabla \cdot \left[\sigma(-\nabla V)\nabla V\right] = 0, \tag{6}$$

$$\mathbf{E} = -\nabla V,\tag{7}$$

where V[V] is the electric potential, E[V/m] is the strength of the electric field, and $\sigma(E)[S/m]$ is the electrical conductivity.

The electrical properties are introduced by material laws eq. (5), as local quantities, functions of space and time. A biological material medium (e.g., a volume of lavender leaves) can be analyzed at the scale of the "application" itself as a continuous, heterogeneous medium, whose properties are correlated (equivalent, effective, mediated) with the material properties of the cells, treated in turn as continuous, heterogeneous media.

If "fine" processes (e.g., membrane's permeabilization)

¹ Doctoral School of Electric Engineering, National University of Science and Technology, Politehnica of Bucharest, Romania.

² Faculty of Electric Engineering, National University of Science and Technology, Politehnica of Bucharest, Romania. E-mails: florin.saftoiu@stud.energ.upb.ro, alexandru.morega@upb.ro, yelda.veli@upb.ro

are treatable at the cellular level, then the processes at the "technological" scale are approached at the global level, without distinguishing cells – they are entities at a different scale (different order of magnitude). Regardless of the approach, the ET analysis requires knowledge of the material properties, obtained through physical or numerical experiments (numerical modeling).

The organic material's properties, considered here as a continuous medium, are established by interpreting, explaining, and evaluating the phenomena that occur at the cellular level during the EP process.

2.1 HOMOGENEOUS PROPERTIES OF THE VOLUME LEVEL OF ORGANIC MATERIAL

The behavior of a volume of organic material in an electric field EP (in conditions where the component cells and their environments cannot be distinguished) can be analyzed by considering the electrical polarization processes at the interfaces between the constituent phases, characterized by different electrical properties (permittivity and electrical conductivity). This phenomenon can be described by analogy with a Maxwell capacitance system [5]. Modeling of material properties at the level of a continuous environment, from nanomaterials to biological systems such as cells or soils, where interfaces separate regions with distinct electrical characteristics, can be achieved using a Maxwell-Wagner model [6-9], which may provide effective values for properties

$$\varepsilon_{eff} = \varepsilon_m \left[1 + 2\phi \frac{\varepsilon_p - \varepsilon_m}{\varepsilon_p + 2\varepsilon_m} \right] / \left[1 - \phi \frac{\varepsilon_p - \varepsilon_m}{\varepsilon_p + 2\varepsilon_m} \right], \quad (8)$$

$$\sigma_{eff} = \frac{\sigma_i \varepsilon_m \sigma_i \varepsilon_m + \sigma_m \varepsilon_p}{\varepsilon_p + \varepsilon_m} \tag{9}$$

where φ is the volume fraction of inclusions (lavender cells), ε_m is the permittivity of the surrounding medium (technological fluid, *e.g.*, water), and ε_p is the permittivity of the inclusion (cell, particle). Table 1 presents values (order of magnitude) of these properties for lavender tissue, as a function of the working frequency, before and after EP.

Table 1
EP parameters, orders of magnitude, bulk properties, and Maxwell-Wagner estimates [10–12].

Frequency [kHz]	Ucritic [kV]	ε_r in general	$\epsilon_{r,eff}$ M-W	σ [S/m] in general	σ _{eff} [S/m] M-W
Before electropermeabilization (bEP)					
< 1	2.53.5	100200	104105	0.010.1	0.0010.01
11000	34	50100	103104	0.11	0.010,1
> 1000	45	2050	102103	110	0.11
After electropermeabilization (aEP)					
< 1	2.53.5	1020	103104	110	0.11
11000	34	510	102103	10100	110
> 1000	45	25	10102	10100	110

The Maxwell-Wagner model produces lower conductivity and higher permittivity than those obtained, for example, experimentally, because the model considers the complex dielectric structure of biological materials, including cell membranes and intracellular and extracellular media.

Table 2

Electrical permittivity and electrical conductivity at an EP cell level. The cell is considered a continuous, homogeneous medium in parts.

EP at 1 kHz (lavender) [13–15].

	σ [S/m]	ε_r	σ [S/m]	ε_r
	Befor	re EP	Afte	r EP
Cell membrane, $\varepsilon_{r,m}$ Cell wall, $\varepsilon_{r,pc}$ Cell cytoplasm, $\varepsilon_{r,cc}$ Essential oil, $\varepsilon_{r,uc}$	10 ⁻⁷ 10 ⁻⁶ 10 ⁻⁶ 10 ⁻⁵ 10 ⁻² 10 ⁻¹ 10 ⁻¹⁰ 10 ⁻⁹	10^210^3 1050 10^310^4 25	10 ⁻⁵ 10 ⁻⁴ 10 ⁻⁵ 10 ⁻⁴ 10 ⁻¹ 1 10 ⁻¹⁰ 10 ⁻⁹	$10^{1}10^{2}$ 1050 $10^{3}10^{4}$ 25

Intracellular space, $\varepsilon_{r,si}$	10-210-1	10^310^4	10-11	10^310^4
-------------------------------------------	----------	------------	-------	------------

The changes in electrical properties after EP are also more pronounced in the Maxwell-Wagner model, because the formation of pores in cell membranes can significantly change the dielectric properties of the tissue. For a plane armature cylindrical capacitor working cell, with the spacing between armatures d=50 mm, the cell diameter D=40 mm. The rectangular pulses (PWM) have a frequency of 1 kHz, $\varepsilon_r=80$ (e.g., Table 2), and the critical voltage is

$$U_{critic} \approx A \varepsilon_r^{\ \alpha} \left(\frac{D}{d}\right)^{\beta},$$
 (10)

where $A \approx 15$ kV is a material constant, $\alpha \approx 0.3$, $\beta \approx 0.8$ are empirically established exponents.

The "threshold" value $\mathbf{E}_{\text{critic}}$, for a two-electrode device, can be established, in the sense of the order of magnitude, by dividing the voltage drop between the electrodes by the distance between them, $\mathbf{E}_{\text{critic}} = U_{\text{critic}}/d$, where U_{critic} is the breakdown voltage. Depending on the working conditions, $\mathbf{E}_{\text{critic}} = function(\sigma, \varepsilon, frequency, temperature) ~300 \text{ kV/m}$.

At the cellular level, EP leads to the formation of transmembrane pores (aqueous channels through lipid membranes), thereby significantly reducing the membrane's electrical resistivity. EP can be reversible, the pores can close, and the membrane can return to its initial state. In these circumstances, electrical conductivity is a nonlinear function of the electric field intensity. In the permeabilized state, the dependence on the working frequency is weaker, especially for lower frequencies. Typically, the applied signal (pulse) has an amplitude in the range 1000 V/cm - O(1) kV/cm, duration O(ms) - O(ms), pulses/second, and the waveform can be rectangular, decreasing exponential, for example [16]. Table 3 summarizes the electrical properties of lavender (continuous medium) used in the modeling of the EP process used in the modeling presented below.

Table 3
Electrical properties of electropermeabilized lavender [16].

Property	Information			
Electrical conductivity, σ	100 mS/m to 1000 mS/m or more. - can increase by 2 - 3 orders of magnitude compared to intact tissue. - depends on the pulse parameters (voltage, duration, frequency).			
Relative permittivity, dielectric constant, ε _r	10 - 30 reduced capacitive effects at the membrane level.			
(decreases due to membrane	20 - 100.			

3. NUMERICAL MODELING OF ELECTROPERMEABILISATION

Next, two fundamental stages of electropermeabilization are analyzed: the permeabilization process, carried out in the presence of an electric field, and the pore-closure stage, which occurs upon suppression of the electric field. The computational domain represents a volume of biological mass, assumed to be a heterogeneous medium, homogeneous within portions, corresponding to the two phases: permeabilized and non-permeabilized [17]. The working cell is a vessel equipped with a pair of electrodes.

The EP cell pre-sizing is performed for the distance between electrodes $d \approx 16$ mm, PWM rectangular voltage wave, $V \approx 6$ V ($\mathbf{E}_{\text{critic}} = V/d = 375$ V/m), PWM period 5 ms, pulse duration 50 μ s, $\sigma_{\text{initial}} = 0.01$ S/m (initial state, non-permeabilized), $\sigma_{\text{max}} = 0.2$ S/m (final state, permeabilized).

3.1 THE ELECTRICAL CONDUCTIVITY IN THE ELECTROPERMEABILIZATION PROCESS

The evolution of the EP process oscillates, with different poration (fast process) and sealing (slow process) speeds, between material permeabilization, during the "on" period of the PWM signal, if the local threshold condition $E > E_{\rm critic}$ is met, and pore closure, during the "off" period of the PWM signal wave, when the threshold condition is no longer met. To model this effect, the electrical conductivity is defined by the ordinary differential equation (ODE),

$$\frac{\partial \sigma}{\partial t} = \begin{bmatrix} k_{open}(\sigma_{max} - \sigma)\Theta(E - E_{crtic}) - \\ -k_{close}(\sigma - \sigma_{initial}) \end{bmatrix}, \quad (11)$$

where k_{open} is the pore formation rate (0.1 s⁻¹), k_{close} is the pore reclosing rate (0.05 s⁻¹), and Θ is the Heaviside function. It is assumed that the dynamics of this process are local, governed solely by the local electric field gradient, with no diffusion.

The duration of the EP process is aligned with the evolution of the electrical conductivity, whose asymptotic, exponential behavior is given by

$$\sigma(t) = \sigma_{max} + (\sigma_{initial} - \sigma_{max})e^{-\frac{k_{open} + k_{close}}{t}}.$$
 (12)

3.3 NUMERICAL MODELING OF THE ELECTRIC CONDUCTIVITY SHIFT IN EP

The mathematical model of the EP process is given by eq. (7) and eq. (11), two boundary and initial condition problems, which are solved simultaneously, numerically, using the finite element method. The computational domain is a cross-section through the work cell, considering that a Cartesian (plane-parallel) model is relevant.

Using geometric and physical symmetry, the model may be reduced to a quarter, which is representative of the analysis of the EP process. Figure 1 shows the actual (reduced) computational domain and the boundary conditions for the four problems that are integrated numerically using the finite element method [18].

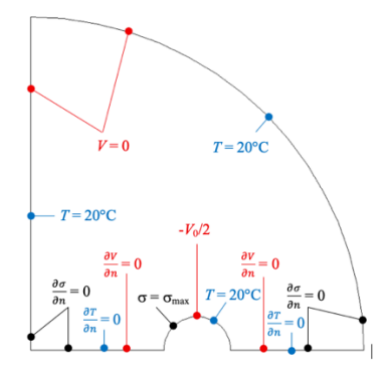


Fig. 1 – The boundary conditions that close the mathematical models.

The boundary conditions for the electromagnetic field problem (7) are established as follows: the electrode surfaces are of the Dirichlet type, $\pm V$ (PWM signal); the enclosure is grounded. The initial state corresponds to the non-permeabilized phase, at 20 °C.

To solve the ODE, eq. (12), we use a general flux-conservative partial differential equation (PDE) model:

$$\frac{\partial f}{\partial t} + \nabla \cdot \left(\underbrace{\frac{\operatorname{diffusion} \quad convection}{\widehat{c}\nabla f} - \underbrace{\alpha f}_{conservative \ flux}^{convertion} + \underbrace{\beta v}_{absorbtion}^{convertion} + \beta \nabla f = \underbrace{g}_{source}, (13)$$

where $f(x,y,t) = \sigma(x,y,t)$ is the unknown, c = 0, a = 0, g = 0, a = 0, b = 0, and the source term, $g = k_{open}(\sigma_{max} - \sigma)\Theta(E - E_{critic}) - k_{close}(\sigma - \sigma_{initial})$, is a function of f(x,y,t).

The boundary conditions for problem (13) are Dirichlet, $f = \sigma_{\text{max}}$, on the electrode surface (it is assumed that the adjacent material permeabilizes as soon as the electrode is activated), and Neumann-type homogeneous elsewhere, Fig. 1. The initial state of the working volume corresponds to a non-permeabilized environment.

The model (11), rewritten as (13), is solved at each point in the computational domain, for each time step. Its integration is used to update the electrical conductivity used in solving the electric field problem (7).

3.3 PROCESUAL HEATING MENACE

A phenomenon associated with the presence of an electric conduction current is the Joule effect, which heats the cell membrane, favoring the formation of pores. The application of a pulsating electric field, consisting of pulses or pairs of pulses ("bursts") at a specific frequency, modifies the cell's thermal state. Numerical simulations show that, up to a certain point, frequency and temperature are directly proportional, but beyond a specific frequency, the temperature decreases; therefore, the frequency-temperature function in the case of electroporation with pairs of pulses is not monotonic [14].

The presence of an electric current results in heating due to the Joule effect. In these circumstances, ensuring the thermal stability of the volume of organic material, within the accepted biological limits, respectively 25 °C - 37 °C [15].

The analysis of thermal working conditions requires solving a heat transfer problem for the volume of biological material considered, here, as a linear, homogeneous, and isotropic medium, with an internal heat source (Joule effect), described by the energy equation:

$$\rho c_p \frac{\partial T}{\partial t} = \nabla \cdot (k \nabla T) + p_{J}, \tag{14}$$

where k [W/m·K] is the thermal conductivity, c_p [J/(kg·K)] is the specific heat, ρ [kg/m³] is the mass density, and $p_J = \sigma^{-1}J^2$ [W/m³] is the power density (Joule source).

Convective effects (heat transfer by thermal motion) are neglected due to the presence of a fluid phase, corresponding to the oil released progressively through the EP.

The boundary conditions are shown in Fig. 1. It is assumed that the electrodes and the cell wall are in contact with a thermostat, which maintains the temperature at 20 °C. A solution is the use of Peltier elements, which can ensure the removal of the heat produced by the EP. The initial thermal state is $T_{\rm initial} = 20$ °C.

In the formulation of the numerical model, to properly represent the transition from a non-permeabilized medium to a permeabilized medium, which occurs at the level of the extremely slender, diffuse interface, higher-order finite elements were used: Lagrange of order IV for the electromagnetic field problem and Lagrange of order V for the electrical conductivity problem. For the other models, second-order Lagrange elements provided accurate results.

The solution of the three coupled "physics" – electric field, eq. (6); the variation of the electrical conductivity as a function of the electric field strength, eq. (11); the heating, eq. (14) – is performed simultaneously, using a segregated solver [18]: at each time step, they are solved successively, iteratively, until

the convergence criterion is satisfied (relative iteration errors, 0.01, absolute iteration errors, 0.001).

4. NUMERICAL SIMULATION RESULTS

4.1 THE ELECTRIC FIELD

The operating mode is transient; the voltage applied to the cell terminals is 6 V; the PWM signal used in these circumstances has a period of 5 ms and an "on" interval of 50 ms. The "off" interval is necessary to restore biological mass and limit EP heating. The process lasts approximately 5...10 min. The electric field is illustrated in Fig. 2. The electric-field spectrum shows no significant, perceptible changes over time.

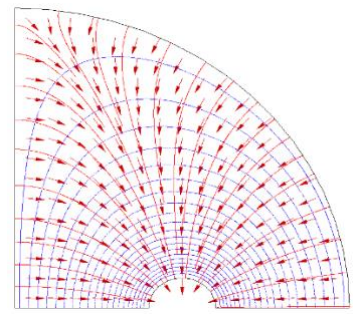


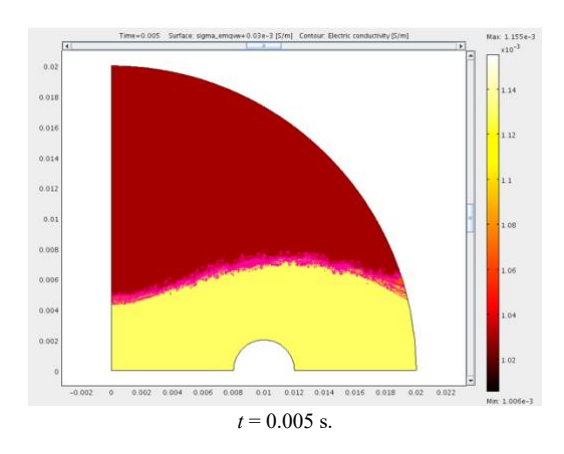
Fig. 2 – Numerical simulation results, the electric field strength presented by field lines and (normalized) vectors (electric field strength), and the electric potential presented with equipotential—circular cell.

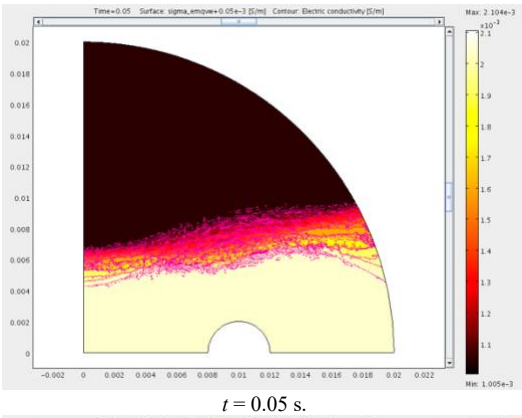
The threshold value of the electric field strength at which EP occurs is 200 V/m. Figure 5 presents, using a color map and contour lines, the variation in electrical conductivity during the EP process at three points in time. The electrical conductivity, in the initial state (non-permeabilized material), is $0.001~\rm S/m$, and in the final state (permeabilized) is $0.2~\rm S/m$. The transition between the two states occurs at a "diffuse" interface (spatial region) where the electric field gradient exceeds the EP $E_{\rm critic}$ threshold.

4.2 THE ELECTRIC CONDUCTIVITY

The emergence of the transition zone between the two states, EP and non-EP, can be accentuated by the model's resolution. Higher-order finite elements (polynomials) were used for representation, which ensures numerical (arithmetic) accuracy within the imposed limits. Clarification of this aspect is the subject of a future stage.

This distribution of electrical conductivity enables the comparison of numerical results with experimental data available in the literature, e.g., [21].





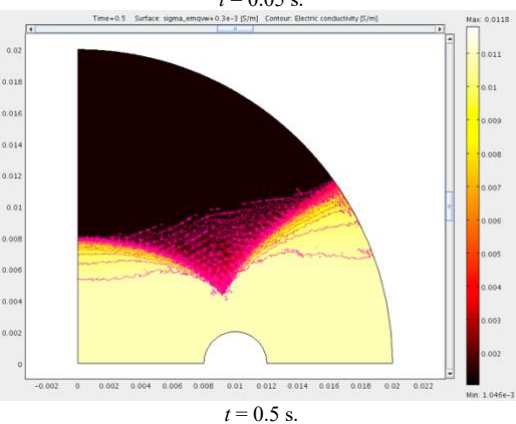


Fig. 3 – Numerical simulation results, electrical conductivity distribution (color map). The EP threshold is set to 200 V/m. Values are in S/m.

Correlating the electrical conductivity map (Fig. 3) with the electric field distribution map (Fig. 2), one can observe the persistence of an area where, during the simulation, no permeabilization occurs. In that region, E, within the numerical modeling parameters, does not exceed the EP threshold. Of course, the applied voltage can be increased, but, from our results, it only reduces the non-permeabilized region, without eliminating it. On the other hand, the electric conduction current density increases, which causes the material to overheat – the Joule effect increases with the square of the current density.

4.3 THE HEAT TRANSFER IN THE ELECTROPERMEABILIZATION PROCESS

The thermal regime of the cell at t=0.5 s during the experiment is shown in Fig. 4. Later, the cell becomes practically isothermal, with a temperature range of 20 °C–20.3 °C, suggesting that the provided cooling ensures good operation. Thermostat devices, such as Peltier coolers, can be used to exhaust heat from electrodes and the cell, keeping them at 20 °C.

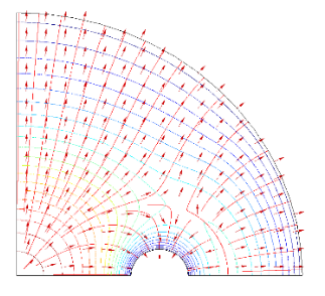


Fig. 4 – Numerical simulation results, the thermal state of the cell: isothermals, field lines, and vectors (normalized) for heat flux density (thermal power) at t = 0.5 s.

A solution to reduce the regions below the EP threshold may be to modify the cell, for example, a cell with an elliptical cross-section.

4.4 THE ELLIPTICAL EP CELL

The threshold electric field strength for EP is 200 V/m (Fig. 5).

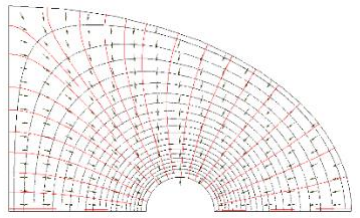
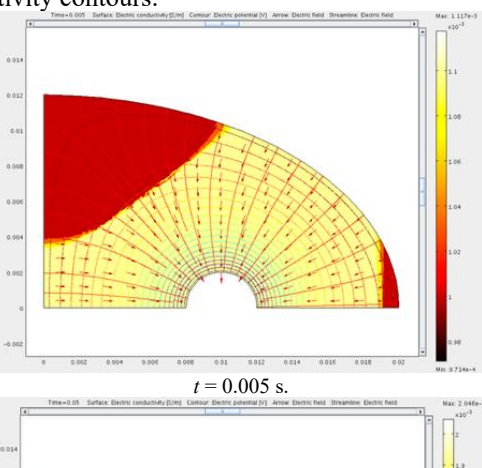


Fig. 5 – Numerical simulation results, the electric field represented by field lines and (normalized) vectors (electric field strength) and equipotential curves, at t = 0.5. Elliptical cell.

Figure 6 illustrates the dynamics of electrical conductivity, presented as a color map and as electrical conductivity contours.



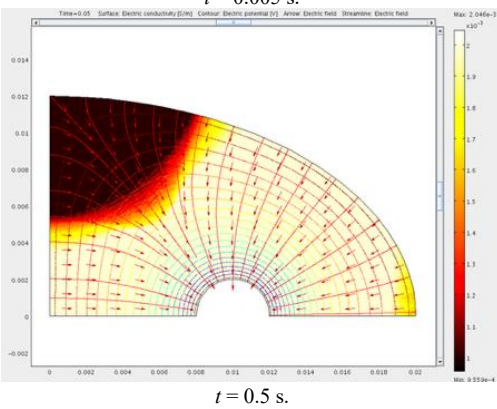


Fig. 6 – Numerical simulation results, electrical conductivity distribution (color map). The EP threshold is set to 200 V/m. Values are in S/m—elliptical cell.

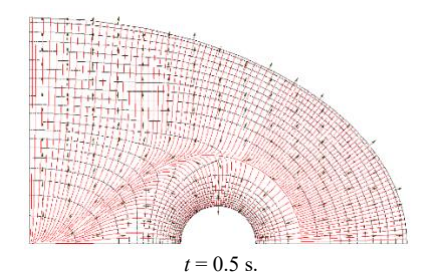


Fig. 7 – The thermal state of the cell: isotherms, field lines, and vectors (normalized) for heat flux density (thermal power).

A better use of the working space in terms of EP can be observed. Modifying the cell section to optimize the EP

volume may be a future research direction. The thermal state of the cell is shown in Fig. 7. After 0.5 s, the cell is practically isothermal at 20 °C - 20.8 °C, suggesting that the provided cooling can ensure good operation.

Another possibility for eliminating areas with an electric field gradient below the EP threshold may be to rotate the electrodes relative to the vessel, thereby temporarily confining areas with low EP potential. In the conceptual model presented below, the rotation frequency is 1.3 Hz, in a counterclockwise direction.

4.5 ELECTROPERMEABILIZATION CELL, ROTARY

For the motion modeling, the FEM mesh discretization technique implemented by [18] is used for the entire cell (circular section): a new boundary problem is solved, in which the rotational motion of the electrodes is given as a boundary condition. For the interior domain, a "freely" deformable (ALE) mesh is established, and the cell wall is immobile. This problem is added to the three (electric field, electrical conductivity, heat transfer) and solved together with them at each time step using the same segregated solver approach.

Figure 8 shows the electric field for the rotating cell at different times. From the initial moment, when the field lines are symmetrical with respect to the two planes of geometric symmetry, until t = 10 s, when it regains the same appearance, its structure changes, preserving only the center-symmetry.

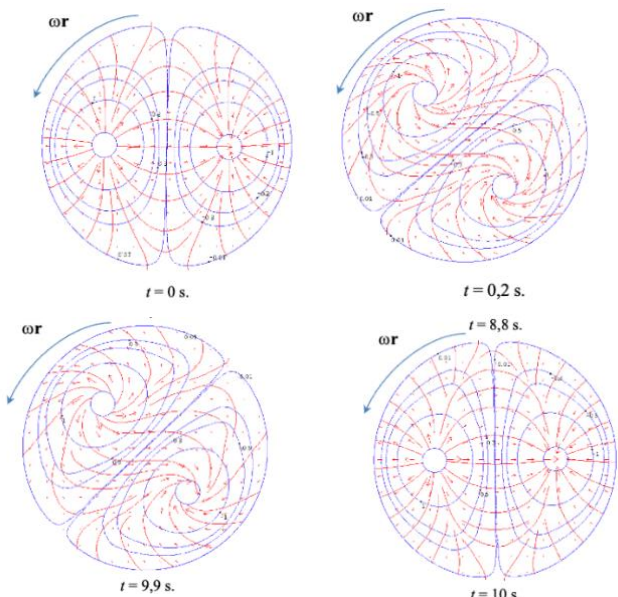
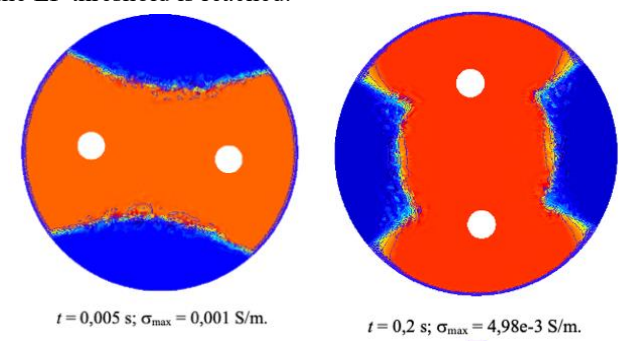
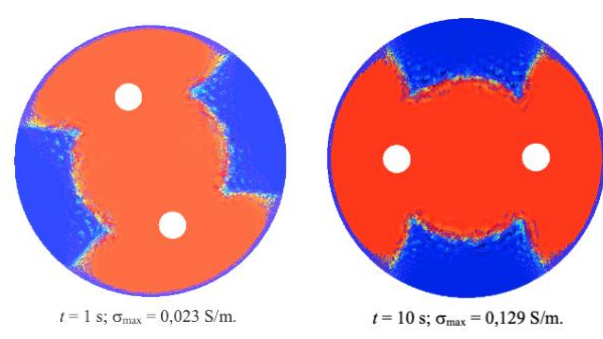


Fig. 8 – The electric field by field lines and (normalized) vectors (electric field intensity) and equipotential curves—rotating circular cell.

Figure 9 shows the electrical conductivity for the rotating cell at different times. It can be observed how, progressively, the still non-permeabilized area is significantly reduced, as the EP threshold is reached.





602

Fig. 9 – The EP process revealed through the electrical conductivity dynamics. Rotating circular cell.

The modification and evolution of the shape and structure of the electric field spectrum can be explained by considering the dynamics of the electrical conductivity distribution: the electrical environment evolves, and the electrical flux "chooses" the path of better electrical conductivity at each moment.

5. CONCLUSIONS

This study aimed to evaluate the impact of the EP cell design – structure, electromagnetic field (EMF), heat transfer, and matrix properties – electric conductivity and electric permittivity. It was revealed that "inactive" electric field regions, where the field is below the critical (threshold) field required for permeabilization, may delay or prevent permeabilization. Areas where the permeabilization conditions persist, and their reduction or suppression, may lead to more efficient EP cells. An elliptical cross-sectional cell performs better than a circular one. Motion-controlled EP enables permeabilization in regions that would otherwise be left out of the EP.

EP depends on the distribution of the electric field, which in turn depends on and, here, determines the material's electrical properties. Some critical value for electric field strength acts as a "switch" of the EP, which is, to some extent, reversible. The cell's thermal state is modulated by the Joule effect, which cannot be suppressed, but can be maintained within acceptable limits by PWM regimes with reduced duty cycles and by active cooling.

The three coupled "physics" – the electric field, the dynamics of electrical conductivity as a function of the electric field intensity, and the heating – are solved simultaneously using a segregated solver. At each time step, they are solved iteratively until the local and per-time-step convergence criteria are satisfied. Their characteristic time scales (EMF and electrical conductivity: fast; heat transfer: slow) are used to inform the solution strategy.

ACKNOWLEDGEMENT

The first author acknowledges the support received during his doctoral studies. His contribution to this work is part of his doctoral thesis. The third author acknowledges support from the National Program for Research of the National Association of Technical Universities – GNAC ARUT 2023.

CREDIT AUTHORSHIP CONTRIBUTION STATEMENT

Florin SĂFTOIU: Documentation, technical and press input data curation and concurrence with experimental results; numerical experiments.

Alexandru M. MOREGA: Physical and mathematical models, numerical implementation.

Yelda VELI: Numerical simulations, postprocessing.

Received on 9 September 2025.

REFERENCES

- T. Kotnik, W. Frey, M. Sack, S. Haberl Meglič, M. Peterka, D. Miklavčič, *Electroporation-based applications in biotechnology*, Trends Biotechnol., 33, 8, pp. 480–488 (Aug. 2015).
- E. Demir, S. Tappi, K. Dymek, P. Rocculi, F. Gómez Galindo, Reversible electroporation caused by pulsed electric field – Opportunities and challenges for the food sector, Trends Food Sci. Technol., 139, p. 104120 (2023).
- K. A. DeBruin, W. Krassowska, Modeling electroporation in a single cell: Effects of field strength and rest potential, Biophys. J., 77, 3, pp. 1213–1224 (Sep. 1999).
- T. Kotnik, G. Pucihar, M. Rebersek, D. Miklavčič, L.M. Mir, Role of pulse shape in cell membrane electropermeabilization, Biochim. Biophys. Acta, 1614, 2, pp. 193–200 (Aug. 2003).
- C.I. Mocanu, Electromagnetic Field Theory, (in Romanian) E.D.P., Bucharest (1982).
- T.T.N. Vu, G. Teyssedre, S. Le Roy, C. Laurent, Maxwell-Wagner effect in multi-layered dielectrics: interfacial charge measurement and modelling, Technologies, 5, 27 (2017).
- H.P. Schwan, Electrical properties of tissue and cell suspensions, Advances in biological and medical physics, 5, pp. 147-209 (1957).
- K.R. Foster, H.P. Schwan, Dielectric properties of tissues and biological materials: a critical review, Critical reviews in biomedical engineering, 17, 1, pp. 25-104 (1989).
- L. Bao, W. Shang, Dielectric Properties of Biological Tissues: A Review. Sensors, 18, 5, 1433, (2018).
- K. Dymek, P. Dejmek, F. Gomez Galindo, Influence of pulsed electric field protocols on the reversible permeabilization of rucola leaves, Food and Bioprocess Technology, 7, 3, pp. 761–773 (2014).
- E. Vorobiev, N. Lebovka, Pulsed-Electric-Fields-Induced Effects in Plant Tissues: Fundamental Aspects and Perspectives of Applications, in Electrotechnologies for Extraction from Food Plants and Biomaterials, Springer, New York, pp. 39–81, NY(2008).
- 12.J. Kulbacka, L.M. Frey, M. Kotulska, Electroporation in biological membranes: Theory and applications, in Advances in Biomembranes and Lipid Self-Assembly, 29, pp. 65–110, Academic Press (2019).
- B. Gabriel, J. Teissié, Direct observation in the millisecond time range of fluorescent molecule asymmetrical interaction with the electropermeabilized cell membrane, Biophysical Journal, 73, 5, pp. 2630–2637 (1997).
- 14. K. Dymek, P. Dejmek, F. Gomez Galindo, Influence of pulsed electric field protocols on the reversible permeabilization of rucola leaves, Food and Bioprocess Technology, 7, 3, 761–773 (2014).
- 15. T.T.N. Vu, G. Teyssedre, S. Le Roy, C. Laurent, Maxwell-Wagner effect in multi-layered dielectrics: interfacial charge measurement and modelling, Technologies, 5, 27 (2017).
- 16. A. Çınar, K. Ateş, L.N.Ö. Polat, S. Elmasulu, I.K. Oğuz, O. Çınar, Ş. Özen, Adulteration control of lavender essential oil by using its electrical properties in the low-frequency range, Measurement Science Review, 25, 3, pp. 141–147 (2025).
- 17. K. Kurata, M. Matsushita, T. Yoshii, T. Fukunaga, H. Takamatsu, Effect of irreversible electroporation on three-dimensional cell culture model, Proc. Annu. Int. Conf. IEEE Eng. Med. Biol. Soc. (EMBC), San Diego, CA, USA, pp. 179–182 (2012).
- 18. ***Comsol a.b., www.comsol.com.
- F. Guo, X. Nie, J. Hong, Y. Zhang, J. Sun, Influence of Joule heating during single-cell electroporation simulation under IRE and H-FIRE pulses, Materials Today Communications, 33, p. 104358 (2023).
- S. Najafian, The effect of time and temperature on the shelf life of essential oils of Lavandula officinalis, J. of Essential Oil Research, 28, 5, pp. 413–420 (2016).
- 21. K. Kurata, M. Matsushita, T. Yoshii, T. Fukunaga, H. Takamatsu, Effect of irreversible electroporation on three-dimensional cell culture model, in Proc. Annu. Int. Conf. IEEE Eng. Med. Biol. Soc. (EMBC), San Diego, CA, USA, pp. 179–182 (2012)